Finite element parametric study of the performance of a deep excavation

Y.P. Dong[a], H.J. Burd[b] & G.T. Houlsby[c]

Abstract: Deep excavations are widely used for the development of underground space. The structural performance of any deep excavation is influenced by details of the soil behaviour, the form of the retaining and support structures that are employed and also the sequence of construction. Finite element analysis is potentially an effective tool for considering both the geotechnical and structural aspects of the design of deep excavations. To capture the main features of the excavation behaviour, a finite element model is required that is able to represent the principal deformation and structural mechanisms at an appropriate level of detail. The current paper explores the various modelling assumptions that need to be considered when developing detailed 3D finite element models for the design of deep excavations. A parametric study is described, based on an idealised square excavation, to investigate the influence that certain key features of the model can have on the quality of the computed results. The study includes the choice of element type to model the structural components, the selection of appropriate material parameters, the choice of procedures to model post-cure shrinkage of the concrete elements and the choice of procedure to model the soil/structure interfaces. The results of this parametric study provide guidance for the development of finite element models for practical design purposes.

Key words: finite element analysis, deep excavations, shrinkage, discontinuities, soil/structure contact

1 Introduction

Deep excavations are widely used in urban areas for the development of underground space. However, the excavation process inevitably alters the stress state in the ground and may cause significant local ground movements to occur. When the excavation is close to existing infrastructure (e.g. buildings, tunnels and buried pipelines), any excavation-induced ground movements must be carefully monitored and controlled to ensure that damage is minimised.

[a]Postdoctoral Associate, Singapore-MIT Alliance for Research and Technology, Singapore, former DPhil student at University of Oxford, UK. Corresponding author.
[b]Associate Professor, Department of Engineering Science, University of Oxford, OX1 3PJ, UK.
[c]Professor, Department of Engineering Science, University of Oxford, OX1 3PJ, UK

The performance of a deep excavation is influenced by a number of issues relating to details of the local soil behaviour, the structural form of the retaining structures and the sequence of construction. Finite element analysis has the potential to be an effective design tool for deep excavations. For the results of any finite element model to be useful, however, careful attention needs to be paid to the choice of constitutive models for the soil and structural elements, the approach used to simulate the construction procedure and modelling procedures for the soil/structure interfaces (e.g. Potts and Zdravkovic, 2001).

Previous research on this topic has demonstrated the importance of several aspects of the modelling process such as: (i) the advantages of 3D analyses over 2D analysis (Gourvenec et al. 2002; Zdravkovic et al. 2005; Lee et al. 2011), (ii) small-strain stiffness nonlinearity of the soil (Simpson 1992; Hashash 1992; Potts & Zdravkovic 2001; Dong et al. 2016), (iii) thermal and shrinkage effects in the concrete floor slabs (St. John et al. 1993; Whittle et al. 1993; Dong et al. 2016), (iv) wall installation effects (Ng et al. 1995; Gourvenec & Powrie 1999; Ng & Yan 1999; Schäfer & Triantafyllidis 2004; Schäfer & Triantafyllidis 2006), (v) soil/structure interface behaviour (Day & Potts 1998; Dong 2014), (vi) joints in the retaining wall (Zdravkovic et al. 2005; Dong et al. 2016), (vii) stiffness reductions in the concrete structural components (St. John et al. 1993; Ou et al. 1998; Dong 2014), (viii) initial stress distribution in the ground (Potts & Fourie 1984; Dong et al. 2016). Neglecting some of these aspects is likely to reduce the accuracy of the analysis. In practice, however, it is difficult to consider all of these aspects in a single analysis, due to the level of complexity which would be required in the model. It is, therefore, relevant to understand the influence of these aspects individually in a parametric study. The current paper describes a set of parametric studies conducted on an idealised excavation. The purpose is to provide experience that may be used to support the development of finite element modelling procedures that are effective and useful for practical design purposes.

Constitutive data are required for the soil, the structural components and the soil/structure interfaces. In practice, uncertainties will exist in the most appropriate parameters for use in the analysis. Parameter selection is therefore also addressed in the current paper.

The particular issues addressed in the current paper are:

1) appropriate choice of element type to model the retaining wall (solid elements or shell elements) and the piles (solid elements or beam elements),

2) selection of appropriate values of operational stiffness for the concrete structural components,
3) choice of method to model thermal effects and post-cure shrinkage in the concrete elements,
4) choice of appropriate modelling procedure for the soil/structure interface behaviour,
5) development of appropriate procedures to model the presence of construction joints or other discontinuities in the retaining walls,
6) investigation of the sensitivity of the computed results to the stiffness and strength properties of the soil.

Various other issues also need to be addressed in the development of finite element models of the behaviour of deep excavations. The issues listed above have been prioritised, however, in the current paper. All calculations described in this paper have been conducted using Abaqus v6.11.

2 Idealised square excavation

2.1 Excavation geometry and construction sequence

The parametric study is based on an idealised square basement excavation (40 m × 40 m in plan, 12 m deep) constructed using a top-down method as illustrated in Figure 1. The excavation is retained by a diaphragm wall (1 m thick, 30 m deep) which is supported by three levels of horizontal floor slabs (150 mm thick) and beams (400 mm × 600 mm in section). The floor slabs and beams are, in turn, supported by circular piles (800 mm in diameter, 30 m deep). The vertical distance between the floor slabs is 4 m and the horizontal span of the beams is 8m. Openings are normally designed in the floor slabs for the purpose of lighting, ventilation, and transport of excavated soils, but these details are excluded in the current model. The construction sequence follows the top-down construction method specified in Figure 2. This excavation configuration is broadly typical of modern urban developments.

2.2 Finite element modelling procedure (basic analysis)

Initially, a finite element model of the deep excavation specified in Figures 1 and 2 is developed, based on modelling assumptions that are regarded as being broadly appropriate. This model is referred to as the ‘basic analysis’, meaning that it includes basic features of an excavation analysis, but that additional features could be added to refine the model. A parametric study is

then conducted in which selected aspects of the basic analysis are adjusted individually. The basic analysis is specified below.

The mesh for the soil and the retaining system is shown in Figure 3. The soil is modelled using hexahedral solid elements C3D8R (linear elements with reduced integration). The beams and piles are modelled using beam elements B31 (linear elements). The floor slabs are modelled with quadrilateral shell elements S4R (linear elements with reduced integration). Linear elements are used in this parametric study, but higher order elements are recommended where more accuracy is required.

As shown in Figure 1, two vertical boundaries have symmetric boundary conditions assigned to them, and the other have roller boundary conditions assigned to them, while the bottom of the mesh is fixed. Tie constraints are used to connect the beams, piles, floor slabs, and the diaphragm wall, representing rigid connections between cast-in-situ reinforced concrete components. In the basic analysis the soil elements are tied directly to the solid elements and beam elements used to represent the retaining wall and piles, respectively. In the parametric study, however, a more detailed interface model is investigated. All the analyses in the paper follow the staged construction sequence specified in Figure 2, via successive calculation steps.

2.3 Material models and input parameters

2.3.1 Soil constitutive model

All calculations are conducted assuming that the soil behaves in an undrained manner, using a total stress analysis. The soil is represented by a multiple yield surface kinematic hardening constitutive model (Houlsby 1999) implemented in Abaqus via a UMAT (Dong 2014). This constitutive model has been previously used to conduct post-construction analyses of a deep excavation in Shanghai Clay (Dong et al. 2016). This model provides a means of representing the small strain non-linear behaviour of soil and includes effects such as hysteresis and dependence of stiffness on recent stress history. The undrained assumption in the analysis is justified by the fact that the permeability of the soil is low (typically 10^{-9} m/s) and the excavation process is relatively short. Although some dissipation of excess pore water pressure is likely to occur during the construction process, it is assumed that these drainage effects are minimal. For entirely undrained analysis of saturated material, a total stress analysis has the advantages of robustness in computation and allows use of undrained shear strength as the defining strength parameter, although it has certain limitations compared to effective stress

analysis (for instance the pore pressure is not explicitly calculated). Further discussion of the total stress approach in the context of undrained analysis of deep excavations is given by Dong et al. (2016).

The soil model uses multiple yield surfaces within the framework of work-hardening plasticity theory. Non-linearity of the small-strain response is achieved using a number of nested kinematic hardening yield surfaces with the same shape as an outer fixed von Mises failure surface. As a stress point moves in stress space and encounters a yield surface as shown Figure 4, the stiffness reduces.

The model is specified by the small strain shear modulus, G_0, the bulk modulus, K, the undrained shear strength, s_u, and a set of non-dimensional parameters, c_i and g_i ($i = 1, n$) (see Figure 4, where n is the number of inner surfaces) that are used to specify the size and hardening characteristics of each of the inner surfaces. The size of each inner surface is $C_i = c_i s_u$ and the tangent shear modulus when the i^{th} surface is active is $G_i = g_i G_0$. A total of nine inner yield surfaces are used in the current analyses, a balance between accuracy and computational efficiency.

The values of c_i and g_i adopted in the current analyses are determined using the procedures described in Dong (2014) and Dong et al. (2016) to provide a match with the stiffness degradation curve (variation of tangent shear modulus with shear strain) determined from previously-published laboratory tests on Shanghai Clay. These data are listed in Table 1.

The undrained shear strength, s_u, in the basic analysis is assumed to increase linearly with depth z below the ground level as $s_u = 20 + 2z$ (with units of kPa and m); this profile is based on a least squares fit of data from recent publications on Shanghai Clay (Dassargues et al. 1991; Liu et al. 2005; Xu 2007; Ng et al. 2012), and is indicated in Figure 5. An alternative, softer, profile $s_u = 0.75 \times (20 + 2z)$ is used for some of the parametric analyses.

The small strain shear modulus G_0 is also assumed in the basic analysis to increase linearly with depth as $G_0 = 1250 \times (20 + 2z)$, with units of kPa and m, based on published data on Shanghai Clay (Cai et al. 2000; Chu et al. 2010; Chen et al. 2011; Gao & Sun 2005; Lou et al.

2007), reproduced in Figure 6. This implies a constant rigidity index $I_r = G_0 / s_u = 1250$. An alternative profile $G_0 = 1000 \times (20 + 2z)$ is used for some of the parametric analyses.

The unit weight of the clay γ_s is assumed to be $18\,kN/m^3$ and the water table is assumed to be at the ground surface. The coefficient of earth pressure at rest $K_0 = \sigma'_h / \sigma'_v$ is assumed to be 0.5, equivalent to $K_0^t = \sigma_h / \sigma_v = 0.778$ in terms of total stresses (Dong 2014).

2.3.2 Support structures

The structural components (i.e. the diaphragm wall, beams, piles, and floor slabs) are assumed to be constructed from reinforced concrete. Their behaviour is specified to be linear elastic, and properties for the intact concrete are assumed as Young's modulus $E = 30GPa$ and Poisson's ratio $v = 0.2$.

Retaining walls are typically constructed as panels, with construction joints between the panels. Following Zdravkovic et al. (2005), Dong (2014), and Dong et al. (2016), the retaining wall is modelled as a cross-anisotropic linear elastic material to take into account the structural influence of the construction joints. For the local coordinate system in Figure 7, the Young's modulus E_2 along the 2-direction is multiplied by an anisotropy factor $\beta, (\beta < 1.0)$, while the material is isotropic in 1-3 plane ($E_1 = E_3$). For the basic analysis $\beta = 1.0$; alternative values of β are adopted in the parametric study.

Thermal effects, associated with the concrete curing process, are included in the analyses by specifying a coefficient of thermal expansion (CTE), and a temperature change ΔT. For the basic analysis $\Delta T = 0$. Alternative values of ΔT are adopted in the parametric study.

3 Parametric study

3.1 Specification of the parametric study

A parametric study has been conducted as shown in Figure 8. The basic analysis is conducted first. The influence of various features of the model is then explored using a series of subsidiary calculations.

Detailed descriptions of the parametric study are presented in the following sections. The results focus principally on the wall deflection at the wall centre and corner (points A and C in

Figure 1) and ground movement behind the wall centre (along line AB in Figure 1) at the final stage of the excavation construction process.

3.2 Choice of element type for the wall and piles

The retaining wall could be modelled with either solid elements or shell elements in a 3D analysis. Shell elements may initially appear to be attractive for this application as (i) the wall thickness is specified as a constitutive parameter and so mesh generation is simpler than when solid elements are used, (ii) they are computationally cheaper due to the smaller number of degrees of freedom, and (iii) internal forces and bending moments can be determined directly from the computational results. However, results given in Zdravkovic et al. (2005) and Dong et al. (2016) indicate that when shell elements are used to model a supported retaining wall, the computed wall displacements are typically larger than when solid elements are employed. This behaviour is associated with the zero thickness of the shell elements; as a consequence of this zero geometric thickness, when shell elements are used to model the retaining wall the beneficial bending moments induced in the wall by the shear stresses acting at the wall/soil interface are not correctly incorporated in the analysis.

Similarly, piles can be modelled with either beam or solid elements. Beam elements provide a relatively simple and practical approach when there are a large number of piles in the analysis, since modelling the detailed geometry of each individual pile is not required in the mesh generation process. Beam elements have the disadvantage, however, that detailed modelling of the soil/pile interface behaviour cannot be included within the analysis (unless special procedures are employed). When solid elements are used to model the piles, the mechanics of the soil/pile interface can be included within the analysis using a conventional contact model. However, the need to model the detailed geometry of each individual pile adds considerably to the complexity of the mesh.

To investigate the merits of using shell elements or solid elements to model the wall and beam or solid elements to model the piles, two additional calculations (E1 and E2) have been conducted as specified in Table 2. The meshes used for these analyses are illustrated in Figure 9. In the E1 analysis, the modelling procedures are the same as those employed in the basic analyses, except that the solid element wall (Figure 3b) is replaced by the use of shell elements to model the wall, as shown in Figure 9b. The E2 analysis is based on the use of solid elements (rather than beams) to model the piles. In all other respects the E2 analysis is based on the same assumptions as the basic analysis. In particular, the pile is tied to the adjacent soil. To conduct

the E2 analysis, new meshes are generated for the soil (Figure 9a) and the supporting structure (Figure 9c) in which the piles are modelled using solid elements.

Results from these analyses, plotted in Figure 10, indicate that the computed wall deflections and ground movements when shell elements are used for the wall (analysis E1) are larger than when solid elements are used to model the wall (basic analysis and E2). This finding is consistent with data from Zdravkovic et al. (2005), Dong (2014), and Dong et al. (2016) and confirms previous work suggesting that solid elements are to be preferred for modelling a retaining wall in this context. Although modelling the piles using beam elements results in slightly larger wall deflection and ground movements (compare analysis E2 with the basic analysis in Figure 10), the difference is seen to be small.

Vertical displacement contours for the ground level floor slab at the final stage of the excavation are shown in Figure 11. These results indicate that differences between the basic and E2 calculations are minimal. This comparison suggests that using beam elements to model the piles provides a convenient and practical approach (at least, when details of the soil/pile contact do not need to be considered).

3.3 Influence of the operational stiffness of structural components

Reinforced concrete retaining walls will inevitably crack as the concrete ages, as a consequence of thermal and curing effects (Puller 2003). Cracks are likely to propagate due to the forces and bending moments set up in the structural elements during the construction process. Ou et al. (1998) compared the wall bending moments calculated from field measurements of strain gauges on reinforcement bars embedded in a diaphragm wall and the wall curvature determined from inclinometer readings. They found that bending moments computed from the strain gauges were generally smaller than those determined from the wall curvature (assuming an un-cracked section). These differences were particularly marked near to the location of the maximum lateral wall deflection, and suggest that cracking of the cross section is likely to have a significant influence on the performance of reinforced concrete support structures.

The operational stiffness (i.e. the value of stiffness accounting for local cracking) of the horizontal support system (i.e. beams, floor slabs, and struts) is likely to be lower than the value determined from the intact concrete Young's modulus. Furthermore, the operational stiffness is likely to change as the excavation proceeds and may be influenced by factors such as workmanship, temperature, cracking and creep in the concrete, misalignment errors, and

bending phenomena caused by heave of the piles (Ou 2006). The operational stiffness of bored piles is also likely to be affected by the construction quality and imperfections in the concrete.

In the finite element model, the second moment of area of the diaphragm wall is determined by the specified thickness. The effect of cracking may be represented in the analysis by using an 'operational' Young's modulus, E_o, given by $E_o = R \cdot E$ (where E is the Young's modulus of the intact concrete and R is a reduction factor). A typical value of reduction factor adopted in previous analyses is $R = 0.8$ (Simpson 1992; St. John et al. 1993; Ou 2006).

In the current parametric study, the reduction factor, $R = 0.5$, is selectively applied to structural components as indicated in Table 3. It should be noted that this is a simplified approach to represent the stiffness of concrete structural components which are assumed to behave in the elastic range.

The results of the parametric study in Figure 12 show that as the operational stiffness of the wall decreases (e.g. compare analysis O1 with the basic analysis) larger wall deflections and ground movements are predicted, while the overall deformation pattern is maintained. For analysis O1 (which is likely to provide a realistic modelling approach for the wall) the largest wall deflection and ground movements are approximately 15% greater than computed in the basic analysis. In analysis O2 (reduced slab and beam stiffness) the wall deflection and ground movements are about 10% greater than those obtained from the basic analysis. Therefore, stiffness reduction of the horizontal system is seen to be less significant than the stiffness reduction of the retaining wall. The wall deflection and ground movements (less than 1mm variation for $R = 0.5$) are relatively insensitive to the variation of pile stiffness (analysis O3), suggesting that any stiffness reduction of the piles would not be expected to have a significant influence on the behaviour of the excavation. The computed wall and ground movements increase by over 30%, when a reduced operational stiffness is used for all the concrete components (compare O4 and the basic analysis).

Adopting a reduced operational stiffness for the structural components has a significant influence on the computed excavation behaviour. Careful consideration should be therefore given to the choice of operational stiffness for the beams, slabs and walls in any practical calculation. The selection of appropriate operational stiffness for a particular design situation may be informed by the results of back analysis calculations on existing structures, combined with engineering judgment.

3.4 Thermal effects and shrinkage in the concrete slabs and beams

The concrete components (diaphragm walls, beams, floor slabs, and piles) may experience thermal shrinkage and expansion, cracking and creep during the curing process (e.g. hydration and thermal effects) and also in the longer term due to the variation of ambient temperature. These phenomena have been addressed by previous researchers, e.g., Whittle et al. (1993), Puller (2003), and Ou (2006), but there remains some uncertainty on how these features of behaviour can best be incorporated in a finite element model.

A related issue is the connection between the horizontal support system (slabs and beams) and the retaining wall. In finite element analyses, the horizontal support system is usually tied to the retaining wall. In practice, however, the connection may not be rigid; rotations might occur and gaps may develop. These mechanisms may lead to additional displacements in the retaining wall and surrounding soil.

A relatively straightforward way of incorporating these various thermal and shrinkage mechanisms in a finite element analysis - explored in the current paper - is to assign an appropriate thermal shrinkage to the relevant structural elements. In any practical application, the appropriate magnitude of thermal shrinkage should be estimated from experience or the back analysis of case histories (e.g. Dong et al. 2016).

Thermal effects are included in the current study by assuming a coefficient of thermal expansion of $10^{-5} / K$ and specifying an appropriate temperature change ΔT. Three separate calculations have been conducted as indicated in Table 4. Analysis T1 is intended to model the shrinkage that occurs due to curing of the concrete that forms the slabs and beams. Analyses T2 and T3 are intended to model the additional effect of seasonal temperature variations. In these two calculations, temperature variations of -20K (analysis T2) and +20K (analysis T3) are applied to the ground level beams and floor slab only; the temperature variations specified in these two calculations are applied in addition to the temperature variation specified for analysis T1. Analyses T2 and T3 represent the case where the ground level remains open to the ambient weather conditions; these analyses provide a simplified approach to estimate the likely influence of seasonal temperature variations.

The results of these analyses, shown in Figure 13, indicate that prescribed thermal effects have a significant effect on the computed wall deflection and ground movements. The results of analysis T1 indicate that a prescribed temperature change of $\Delta T = -10K$ causes an

approximately 15% increase in computed wall deflection and ground movements. When additional seasonal temperature changes are incorporated in the analysis (T2 and T3), the wall deflection varies by around 2mm close to the level of the ground level floor slab.

The results of analyses T2 and T3 indicate significant wall and ground displacements in response to seasonal variations in the temperature of the ground level slab. These computed seasonal movements are consistent with field data for a diaphragm wall-supported deep excavation in Boston, U.S., reported in Whittle et al. (1993). In these field data, 5 to 10 mm observed wall movements were judged to be associated with a +25 K ambient temperature change, from February to July. However, in cases where the ground floor slab is enclosed, wall and ground movements due to seasonal temperature variations are likely to be significantly lower in magnitude than those predicted in the current paper.

3.5 Influence of the soil/structure interface behaviour

In deep excavations, there are large areas of interface between the soil and the support structures (i.e. the soil/wall interface and the soil/pile interface). The behaviour at these interfaces is likely to affect the overall excavation performance. In the basic analyses, tie constraints are applied at the soil/structure interfaces, representing a perfectly adhering interface. However, this assumption is unlikely to provide an accurate representation of actual interface conditions.

The soil/structure interface shear resistance is likely to be less than the intrinsic strength of the soil, and will depend on the roughness of the interface. During shearing, the strength of the soil/structure interface typically drops after a peak strength is reached, because the plane surface facilitates the reorientation of soil particles and the destruction of bonds between particles. The actual interface shear resistance is therefore likely to be different from the intrinsic residual strength of the soil. The residual strength on the interface is mobilised after the application of large shear displacement, and depends mainly on the interface roughness, the soil properties, the grain size distribution and shape of the soil particles, the magnitude of the normal stress, and the rate of shear displacement (Lemos and Vaughan 2000).

Understanding the shear strength of the soil/structure interface is important in determining appropriate interface properties to specify in the model. During the installation of diaphragm walls and bored piles, the adjacent soil will suffer a certain amount of disturbance. The soil at the soil/structure interface is assumed to have been sheared to critical state conditions with

operational undrained shear strength $\bar{s}_u = \alpha \cdot s_u$, where α is a reduction factor, and s_u is the *in situ* undrained shear strength. Appropriate values of α for use in practice are often related to the remoulded strength, and are therefore related to the sensitivity S_t.

In the parametric study described in this section, an extended version of the classical isotropic Coulomb friction model (implemented in Abaqus), is used to model the contact between the soil and the structure. The standard Coulomb friction model assumes that no relative motion occurs if the equivalent frictional stress $\tau_{eq} = \sqrt{\tau_1^2 + \tau_2^2}$ (where τ_1 and τ_2 are shear stresses on the interface in two orthogonal directions), is less than the critical shear stress $\tau_{crit} = \mu p$ (where μ is the friction coefficient and p is the local contact pressure). The standard Coulomb model is extended in the current work such that a limit is placed on the critical shear stress, $\tau_{crit} = \min(\mu p, \tau_{\max})$, where $\tau_{\max}$ is a user-specified constant. If the equivalent stress reaches the critical stress ($\tau_{eq} = \tau_{crit}$), slip will occur (see Figure 14). Hard contact is specified in the normal direction of the interface, in which the contact pressure between two surfaces at a point, $p = 0$, when the overclosure of the surfaces, $h < 0$ (gap open), while $p > 0$ when $h = 0$ (gap closed).

The value of $\tau_{\max}$ is linked to the local undrained shear strength of the soil, s_u, by $\tau_{\max} = \alpha \cdot s_u$, where α is a strength reduction factor and s_u is the local value of soil undrained shear strength. Further modification has been made in Abaqus through a subroutine FRIC to allow $\tau_{\max}$ to vary with s_u (since in the version of Abaqus used for the current study, $\tau_{\max}$ can only be specified as a constant). This modified version of the extended Coulomb friction model is illustrated in Figure 14. It is assumed that the critical shear resistance τ_{crit} is limited only by $\tau_{\max}$ in undrained analysis (independent of the coefficient of friction μ), and therefore in the current calculations a large value $\mu = 1000$ is specified. The influence of α on the excavation behaviour is investigated through parametric studies described below.

To include this contact model at the soil/pile interface, the piles are modelled with solid elements (as shown in Figure 9c). It is convenient at this stage to introduce a new reference analysis, based on the basic analysis but with the piles modelled with solid elements (rather than beams) that are tied to the adjacent soil; this analysis is referred to as 'basic analysis (PS)' (where PS signifies that the pile is modelled with solid elements). This analysis is, in fact identical to E2. Later discussion of the results obtained from other parametric study analyses

involving solid elements for the piles make consistent use of comparisons with basic analysis (PS).

3.5.1 Influence of the soil/wall interface properties

Four analyses, specified in Table 5, have been conducted to investigate the influence of soil/wall interface properties on the computed behaviour, and to understand the sensitivity of the results to the value of α. In these analyses the piles are analysed as solid elements, tied to the adjacent soil.

The results, shown in Figure 15, indicate that, as expected, the computed wall deflections and ground movements are sensitive to the soil/wall interface model. The basic analysis (PS) provides a lower bound to the computed movements, suggesting that a tie constraint at the wall/soil interface is likely to give unrealistically stiff results. The data in Figure 15 indicate that the tied (basic analysis (PS)) and smooth (W4) conditions provide bounds on the rough interface results (W1, W2 and W3). The behaviour of a real excavation is likely to lie between these two bounds, depending on the interface properties. These results suggest that careful consideration needs to be given to the choice of α in any practical analysis. The selection of α for a particular design case is likely to be informed by local experience on the nature of the soil/concrete interfaces.

3.5.2 Influence of the soil/pile interface properties

A similar set of analyses has been conducted (specified in Table 6), to investigate the influence of soil/pile interface properties on the excavation behaviour. In a practical design situation, modelling individual piles using solid elements may be impractical, as a consequence of the detailed mesh generation that would be required. This parametric analyses provides information on the extent to which soil/pile contact behaviour can be ignored (in which case using beam elements to model the piles may be an appropriate option).

The results in Figure 16 indicate that the excavation behaviour is sensitive to the soil/pile interface properties; employing a tied contact (basic analysis (PS)) leads to a stiffer response (i.e. smaller ground and wall movements) than computed using contact models where a shear strength is assigned to the interface. The influence of soil/pile interface behaviour is less significant, however, than the influence of soil/wall interface characteristics that is apparent from the results in Section 3.5.1.

The contours of the vertical displacement at the ground level slab from the tied (basic analysis (PS)) and smooth (P4) soil/pile contact conditions are shown in Figure 17. In these results, the pile heads all move vertically upwards during the excavation process, even for the smooth interface case (P4), which is consistent with the field observations described in Xu (2007) . However, the soil/pile contact conditions affect the magnitude of the vertical displacement of the piles and the horizontal support system.

The maximum computed heave at the top of the piles for basic analysis (PS) (tied pile/soil interface) is 13.0 mm. For analysis P4 (smooth interface) the maximum heave is 5.0mm. For intermediate values of interface strength, the maximum computed pile heave is 11.0 mm (analysis P1, $\alpha = 1.0$), 9.1 mm (analysis P2, $\alpha = 0.5$), and 7.2 mm (analysis P3, $\alpha = 0.1$). Heave of the piles may induce additional strains/stresses at the joints between the piles, the beams and the floor slabs. Detailed consideration of these local effects, however, is beyond the scope of the paper.

3.5.3 Combined influence of the soil/wall and soil/pile interface properties

A further parametric study, specified in Table 7, has been conducted in which the influence of soil/structure interface behaviour is investigated for the case where the soil/wall and soil/pile interface are assumed to have the same value of α . The computed results, shown in Figure 18, indicate that the combined influence is larger than the individual influence of either soil/wall or soil/pile interface behaviour. The combined influence approximates to the superposition of the individual effects.

The analyses in the previous sections indicate that (i) the soil/structure interface behaviour has a significant influence on the excavation behaviour and (ii) the influence of the soil/wall contact model is larger than that of the soil/pile contact model. If a rigid connection between the soil and the structure is employed then the results may underestimate the actual deformations. Therefore, the soil/structure interface behaviour should be considered appropriately in the analyses, and the interface properties should be carefully estimated. For practical design calculations, it is suggested that parametric studies on the interface properties (e.g. fully rough and smooth conditions) are conducted to explore the sensitivity of the results to variations in the soil/structure interface models.

3.6 Influence of construction joints in the diaphragm wall

All the analyses described above treat the diaphragm wall as an isotropic elastic material. This approach has been adopted by previous researchers e.g., Simpson (1992), Whittle et al. (1993), Ou et al. (2000). In reality, however, a diaphragm wall is composed of discrete wall panels. The diaphragm wall is discontinuous in the horizontal direction and consequently cannot sustain any significant out-of-plane bending moment about a vertical axis. Moreover, the horizontal axial stiffness of the retaining wall is smaller than the vertical stiffness (Zdravkovic et al. 2005).

In the parametric study described in this section, the wall is represented by an anisotropic model in which the Young's modulus along the wall length direction (E_2 as shown in Figure 7) is multiplied by anisotropy factor $\beta, (\beta \leq 1.0)$. In all other respects, the basic analysis modelling approach is adopted. Four analyses are conducted, as indicated in Table 8.

Zdravkovic et al. (2005) used an anisotropy factor of $\beta = 10^{-5}$ to model a contiguous pile wall (which has relatively weak connections between adjacent piles). The diaphragm wall that is being modelled in the current study is stiffer (in the longitudinal direction) than a contiguous pile wall, and the appropriate value of β is therefore expected to be greater than this value.

As shown in Figure 19, when an anisotropic model is used for the wall, the lateral displacements increase substantially at the wall corner (Point C) whereas the lateral displacements at the wall centre (Point A) are less sensitive to the value of β. Data from field measurements (Xu 2007) suggest that at the corners of an excavation the pattern of wall deformations is similar to those that occur in the centre of the wall, but the general magnitude of the deformations are reduced. This behaviour is captured by the anisotropic wall results in Figure 19.

The anisotropic wall modelling approach also modifies the vertical ground movement distributions, as shown in Figure 20. When $\beta = 10^{-5}$ (analysis A4), the ground settlements at the corner of the excavation become similar to those that develop behind the centre of the wall.

3.7 Influence of the stiffness and strength properties of the soil

Uncertainties typically exist in the stiffness and strength parameters that should be used to represent the soil in any practical design scenario. The strength and stiffness profiles adopted

in the basic analyses are based on previously-published data on Shanghai Clay. To investigate the way in which the assumed soil parameters influence the computed results, three analyses, specified in Table 9 have been conducted. These calculations are based on different linear variations of strength and stiffness with depth. Smaller values than the basic analysis are selected because they tend to produce larger (i.e. more conservative) results. In analysis S1, only G_0 is reduced; in S2, only s_u is reduced; in S3, both G_0 and s_u are reduced (which is likely to be the worst condition). In all other respects, the basic analysis modelling approach is adopted.

As shown in Figure 21, both the wall deflection and ground movements increase significantly when smaller values of G_0 and s_u are used. Smaller values of G_0 lead to larger displacements due to stress changes in the soil, while smaller s_u values result in greater deformation because more soil elements yield and experience plastic deformation. The results of S3 cannot be obtained by simple superposition of the changes observed in S1 and S2. This indicates that the input parameters for both the soil stiffness and strength properties should be carefully calibrated through reliable site investigations to obtain reliable results.

4 Suggested approaches for practical analyses

Suggestions are made, below, on assumptions and choices that might be suitable for the development of 3D finite element models for use in the design of deep excavations in a practical context. Ideally, all of the key features investigated in this paper should be included within the model. However, this may not always be feasible due to limitations e.g. in the capability of the available software, the experience of practitioners, and the available time and computational resources. Three possible approaches for practical analysis (specified in Table 10) are described below. The features adopted in these analyses have been selected, based on the results of the parametric study, to provide procedures that are likely to give reasonable results for practical design purposes.

Analysis F1 considers all the important features addressed in the current paper and is assumed to be the premium analysis. The diaphragm wall and piles are modelled with solid elements, with an interface model used to describe the soil/wall and soil/pile interface properties ($\tau_{\max} = 0.5 s_u$). The stiffness of the reinforced concrete components is reduced to half of the nominal stiffness ($R = 0.5$) to model the influence of imperfections in the concrete. Concrete thermal shrinkage is considered during curing process ($\Delta T = -10K$) and the influence of the

ambient temperature change (winter) is incorporated (by the additional application of $\Delta T = -20K$ to the ground level beams and floor slabs). The diaphragm wall is modelled as a cross anisotropic linear elastic material ($\beta = 10^{-2}$) to include the effect of construction joints.

Analysis F2 uses beams elements to model the piles; this excludes the possibility of a detailed model of the soil/pile interface behaviour (e.g. as incorporated in F1). This case is regarded as being more feasible for a design context because modelling piles with solid elements (as is the case in analysis F1) typically leads to complex mesh generation tasks and a mesh with a relatively large number of degrees of freedom.

Analysis F3 is similar to F1 except that the soil is assumed to be fully bonded to the structural elements. This avoids the need to include a soil/structure contact model within the analysis.

As shown in Figures 22 and 23, significant differences are seen between the results of the improved analyses (F1 to F3) and the basic analysis, indicating the importance of considering the various modelling aspects addressed in this paper. The effect of the soil/pile contact is seen to be minimal (the results of F2 are similar to those of F1). However, the soil/wall contact model is seen to have a significant effect on the computed results (compare F3 with F1). These results suggest that particular care should be taken, when developing models for use in design, to ensure that a realistic model is used for the soil/wall interface behaviour.

5 Conclusions

In any practical design process for a deep excavation, uncertainties typically exist on the most appropriate choices for the various modelling assumptions that need to be embedded in the analysis. The parametric studies described in this paper have investigated, for one particular excavation geometry, the sensitivity of the computed deformations to a variety of modelling assumptions.

General conclusions from the study are summarised below.

1) Retaining walls can be modelled either with solid or shell elements. As a consequence of the fact that the shells have zero geometric thickness, beneficial bending moments resulting from the shear stress acting on the back of the wall (which act to reduce the wall deflection towards the excavation) do not develop in the analysis. Consequently,

the computed wall deflection and ground movement are smaller than those obtained when the wall is modelled with solid elements. Solid elements are therefore regarded as the preferred approach for modelling the retaining wall.

2) Beams elements are regarded as a convenient practical approach to model piled foundations. The task of mesh generation, using beam elements, is considerably simpler than is the case when solid elements are used. The current study indicates that the computed performance of the retaining wall is relatively insensitive to the modelling approach adopted for the piles. Therefore, beam elements are recommended as a practical approach to model the piles in analyses of this sort. However, in cases where detailed soil/pile interaction behaviour needs to be modelled (e.g. to obtained refined estimates of pile heave effects) then resort may be needed to using solid elements to represent the piles.

3) The computed wall deflections and ground movements are sensitive to the operational stiffness of the concrete structural components (which may be smaller than their nominal stiffness due to cracking and other imperfections in the concrete). Parametric studies indicate that the choice of operational stiffness of the wall and horizontal slabs and beams has a significant effect on the magnitude of the computed wall deflection and ground movements, whereas the stiffness of the piles has little effect on the computed performance. Therefore, the operational stiffness of the retaining wall and horizontal system should be selected carefully in the finite element analysis for design purposes.

4) Thermal effects in the concrete horizontal support system (i.e. beams and floor slabs) that develop during the curing process and due to ambient temperature changes have a significant influence on the magnitude and pattern of the computed wall deflections and

ground movements. These thermal effects can be included in the analyses in a straightforward way. The thermal shrinkage of concrete beams and floor slabs during the curing process will act to reduce the support provided to the diaphragm wall. This will cause the diaphragm wall to move towards the excavation with a consequential increase in wall deflection and ground movement. The amount of shrinkage needs to be estimated and specified in the analysis via an appropriate temperature change. Ambient seasonal temperature changes are assumed to affect mainly the ground level floor slabs. Parametric studies indicate that the thermal shrinkage and expansion of the ground level slab principally influences the wall deflection close to the top of the wall and the local horizontal ground movement, whereas the vertical ground movement is relatively unaffected. Careful consideration needs to be given to the choice of appropriate thermal parameters in any practical calculation.

5) The soil/structure interface behaviour is shown to have a significant influence on the excavation performance in the parametric studies. The soil/wall contact is more significant than the soil/pile contact. Neglecting the interface behaviour will cause the deformations to be underestimated.

6) The influence of construction joints in the retaining wall can be included in the analysis by using an anisotropic model for the wall. The computed deformations at the corner of the excavation are seen to be sensitive to the anisotropy factor adopted for the wall. The appropriate value of the anisotropy factor, β, is likely to depend on the nature of the wall (appropriate values of β for a contiguous piled wall are expected to be smaller, for example, than for a diaphragm wall). For practical applications, the value of β should be carefully selected, based on experience and back analysis of case histories.

7) The numerical results are sensitive to the input parameters for the stiffness and strength

properties of the soil. Both the wall deflection and ground movements increase significantly when smaller values of G_0 and s_u are used.

8) In any practical design, it may not be possible to include detailed models of all the features that are relevant to the performance of a deep excavation. The parametric study demonstrates, however, that the results of the analysis are more sensitive to some of the assumptions and parameters than others. This provides a rational basis for decisions on the level of complexity to be employed in the development of 3D finite element models for the design of deep excavations.

6 Acknowledgement

The first author was supported by the China Scholarship Council to study at Oxford University. The calculations were conducted at the Oxford Supercomputing Centre.

7 References

Cai, H., Zhou, J. & Li, X., 2000. Plastoelastic response of horizontally layered sites under multi-directional earthquake shaking. *Tongji Daxue Xuebao/Journal of Tongji University*, 28(2), pp.177–182.

Chen, Q.S., Gao, G.Y. & Yang, J., 2011. Dynamic response of deep soft soil deposits under multidirectional earthquake loading. *Engineering Geology*, 121(1–2), pp.55–65.

Chu, F., Li, Y. & Liang, F., 2010. Numerical analysis of deformation of deep excavation adjacent to metro considering small-strain stiffness of soil. *Yanshilixue Yu Gongcheng Xuebao/Chinese Journal of Rock Mechanics and Engineering*, 29(SUPPL. 1), pp.3184–3192.

Dassargues, A., Biver, P. & Monjoie, A., 1991. Geotechnical properties of the Quaternary sediments in Shanghai. *Engineering Geology*, 31(1), pp.71–90.

Day, R.A. & Potts, D.M., 1998. The effect of interface properties on retaining wall behaviour. *International Journal for Numerical and Analytical Methods in Geomechanics*, 22(12), pp.1021–1033.

Dong, Y., 2014. *Advanced Finite Element Analysis of Deep Excavation Case Histories*. DPhil thesis, University of Oxford, Oxford, UK.

Dong, Y., Burd, H.J. & Houlsby, G.T., 2016. Finite element analysis of a deep excavation case history. *Géotechnique*, 66(1), pp.1–15.

Gao, F. & Sun, X., 2005. Characteristic analysis of Shear wave velocity of foundation ground in Shanghai region. *Shanghai Geology*, 94(2), pp.27–29.

Gourvenec, S., Powrie, W. & Moor, E.K. De, 2002. Three-dimensional effects in the construction of a long retaining wall. *Proceedings of the ICE - Geotechnical Engineering*, 155, pp.163–173.

Gourvenec, S.M. & Powrie, W., 1999. Three-dimensional finite-element analysis of diaphragm

wall installation. *Géotechnique*, 49(6), pp.801–823.
Hashash, Y.M.A., 1992. *Analysis of deep excavations in clay*. Sc.D thesis, Massachusetts Institute of Technology, Cambridge, Boston, U.S.
Houlsby, G.T., 1999. A model for the variable stiffness of undrained clay. In *Proceedings of the International Symposium on Pre-Failure Deformations of Soil*. Torino, pp. 443–450.
St. John, H.D. et al., 1993. Prediction and performance of ground response due to construction of a deep basement at 60 Victoria Embankment. *Predictive soil mechanics. Proc. of the Wroth memorial symposium, Oxford, 1992*, pp.581–608.
Lee, F.H. et al., 2011. Application of Large Three-Dimensional Finite-Element Analyses to Practical Problems. *International Journal of Geomechanics*, 11(6), pp.529–539.
Liu, G.B., Ng, C.W.W. & Wang, Z.W., 2005. Observed performance of a deep multistrutted excavation in Shanghai soft clays. *Journal of Geotechnical and Geoenvironmental Engineering*, 131(8), pp.1004–1013.
Lou, M., Li, Y. & Li, N., 2007. Analyses of the seismic responses of soil layers with deep deposits. *Frontiers of Architecture and Civil Engineering in China*, 1(2), pp.188–193.
Ng, C.W.W. et al., 1995. An approximate analysis of the three-dimensional effects of diaphragm wall installation. *Géotechnique*, 45(3), pp.497–507.
Ng, C.W.W. et al., 2012. Ground deformations and soil-structure interaction of a multi-propped excavation in Shanghai soft clays. *Géotechnique*, 62(10), pp.907–921.
Ng, C.W.W. & Yan, R.W.M., 1999. Three-dimensional modelling of a diaphragm wall construction sequence. *Géotechnique*, 49(6), pp.825–834.
Ou, C.Y., 2006. *Deep Excavation: Theory and Practice*, London: Taylor & Francis.
Ou, C.Y., Liao, J.T. & Lin, H.D., 1998. Performance of diaphragm wall constructed using top-down method. *Journal of Geotechnical and Geoenvironmental Engineering*, 124(9), pp.798–808.
Ou, C.Y., Shiau, B.Y. & Wang, I.W., 2000. Three-dimensional deformation behavior of the Taipei National Enterprise Center (TNEC) excavation case history. *Canadian Geotechnical Journal*, 37(2), pp.438–448.
Potts, D. & Zdravkovic, L., 2001. *Finite Element Analysis in Geotechnical Engineering: Application, Vol. 2*, London: Thomas Telford Limited.
Potts, D.M. & Fourie, A.B., 1984. Behaviour of a propped retaining wall: Results of a numerical experiment. *Géotechnique*, 34(3), pp.383–404.
Puller, M., 2003. *Deep Excavations: a practical manual* Second edi., London: Thomas Telford.
Schäfer, R. & Triantafyllidis, T., 2004. Modelling of earth and water pressure development during diaphragm wall construction in soft clay. *International Journal for Numerical and Analytical Methods in Geomechanics*, 28(13), pp.1305–1326.
Schäfer, R. & Triantafyllidis, T., 2006. The influence of the construction process on the deformation behaviour of diaphragm walls in soft clayey ground. *International Journal for Numerical and Analytical Methods in Geomechanics*, 30(7), pp.563–576.
Simpson, B., 1992. Retaining structures: displacement and design. *Géotechnique*, 42(4), pp.541–576.
Whittle, A.J., Hashash, Y.M.A. & Whitman, R. V, 1993. Analysis of deep excavation in Boston. *Journal of Geotechnical Engineering - ASCE*, 119(1), pp.69–90.
Xu, Z.H., 2007. *Deformation Behaviour of Deep Excavations supported by Permanent Structure in Shanghai Soft Deposit*. PhD thesis, Shanghai Jiao Tong University, Shanghai, China.
Zdravkovic, L., Potts, D.M. & St. John, H.D., 2005. Modelling of a 3D excavation in finite element analysis. *Géotechnique*, 55(7), pp.497–513.

List of notation

CTE - coefficient of thermal expansion

c_i, g_i - non-dimensional parameters in the soil model to define the size and work hardening characteristics of each inner yield surface

E_o - operational Young's modulus

E - Young's modulus of intact concrete

E_1, E_2, E_3 - Young's modulus in the 1-, 2-, and 3-direction, respectively.

G - shear modulus

G_0 - Small-strain shear modulus

I_r - rigidity index

i - the i^{th} inter yield surface of the soil model

K - bulk modulus

K_0 - coefficient of lateral earth pressure at rest in terms of effective stresses

K_0^t - coefficient of lateral earth pressure at rest in terms of total stresses

n - number of yield surfaces used in the soil model

p - pressure on the interface

ΔT - temperature change

R - reduction factor for stiffness

s_u - *in situ* undrained soil shear strength

$\overline{s}_u$ - operational undrained shear strength

z - depth below the ground

α - reduction factor for soil strength

β - anisotropy factor

γ_s - unit weight of the soil

μ - frictional coefficient

ν - Poission's ratio

σ_h, σ_v - total horizontal and vertical normal stress in the soil

$\sigma_h^{'}, \sigma_v^{'}$ - effective horizontal and vertical normal stress in the soil

τ_1, τ_2 - shear stresses on the interface along 1- and 2-direction, respectively

τ_{crit} - critical shear stress on the interface

τ_{eq} - equivalent frictional shear stress on the interface

$\tau_{\max}$ - maximum allowed shear stress at the interface

Table 1. Parameters for the multiple yield surface kinematic hardening model for $n = 9$

n	0	1	2	3	4	5	6	7	8	9
g_i	0.996	0.9	0.7	0.5	0.3	0.15	0.075	0.03	0.0075	0.00058
c_i		0.005	0.0952	0.2264	0.3537	0.5358	0.6769	0.7678	0.8708	0.942

Table 2. Parametric study on element type to model wall and piles

Analysis	**Wall**	**Piles**
Basic analysis	Solid elements	Beam elements
E1	Shell elements	Beam elements
E2	Solid elements	Solid elements

Table 3. Parametric study on operational stiffness

Analysis	**Wall**	**Slabs and beams**	**Piles**
Basic analysis	$R = 1$	$R = 1$	$R = 1$
O1	$R = 0.5$	$R = 1$	$R = 1$
O2	$R = 1$	$R = 0.5$	$R = 1$
O3	$R = 1$	$R = 1$	$R = 0.5$
O4	$R = 0.5$	$R = 0.5$	$R = 0.5$

Table 4. Parametric study on thermal effects and shrinkage. Analysis T2 (winter) and T3 (summer) are intended to model the effect of seasonal variations in ambient temperature

Analysis	**Analysis description**
Basic analysis	No thermal effects
T1	$\Delta T = -10K$ is applied to all beams and slabs. This case is intended to model the effects of concrete shrinkage during the curing process.
T2	$\Delta T = -10K$ is applied to all beams and slabs. To model seasonal variations in ambient temperature an additional $\Delta T = -20K$ is applied to the ground level beams and floor slab.
T3	$\Delta T = -10K$ is applied to all beams and slabs. To model seasonal variations in ambient temperature an additional $\Delta T = +20K$ is applied to the ground level beams and floor slab.

Table 5. Parametric study on soil/wall interface properties

Analysis	**Analysis description**
Basic analysis (PS)	Tied soil/wall and soil/pile interface, solid elements for the piles
W1	Only soil/wall contact included, $\tau_{\max} = \alpha \cdot s_u, \alpha = 1.0$
W2	Only soil/wall contact included, $\tau_{\max} = \alpha \cdot s_u, \alpha = 0.5$
W3	Only soil/wall contact included, $\tau_{\max} = \alpha \cdot s_u, \alpha = 0.1$
W4	Fully smooth contact for soil/wall interface only

Table 6. Parametric study on soil/pile interface properties

Analysis	Analysis description
Basic analysis (PS)	Tied soil/wall and soil/pile interface, solid elements for the piles
P1	Only soil/pile contact included, $\tau_{\max} = \alpha \cdot s_u, \alpha = 1.0$
P2	Only soil/pile contact included, $\tau_{\max} = \alpha \cdot s_u, \alpha = 0.5$
P3	Only soil/pile contact included, $\tau_{\max} = \alpha \cdot s_u, \alpha = 0.1$
P4	Fully smooth contact for soil/pile interface only

Table 7. Parametric study on combined pile/soil and wall/soil interface properties

Analysis	Analysis description
Basic analysis (PS)	Tied soil/wall and soil/pile interface, solid elements for the piles
WP1	Both soil/wall and soil/pile contact included, $\tau_{\max} = \alpha \cdot s_u, \alpha = 1.0$
WP2	Both soil/wall and soil/pile contact included, $\tau_{\max} = \alpha \cdot s_u, \alpha = 0.5$
WP3	Both soil/wall and soil/pile contact included, $\tau_{\max} = \alpha \cdot s_u, \alpha = 0.1$
WP4	Fully smooth contact for soil/wall and soil/pile interface

Table 8. Parametric study on wall anisotropy

Analysis	Analysis description
Basic analysis	Isotropic wall approach, $\beta = 1$
A1	Anisotropic wall approach, $\beta = 10^{-1}$
A2	Anisotropic wall approach, $\beta = 10^{-2}$
A3	Anisotropic wall approach, $\beta = 10^{-3}$
A4	Anisotropic wall approach, $\beta = 10^{-5}$

Table 9 Parametric study on soil properties. Values of *z* are in units of metres.

Analysis	Strength (kPa)	Stiffness (MPa)
Basic analysis	$s_u = (20 + 2z)$	$G_0 = 1.25 \times (20 + 2z)$
S1	$s_u = (20 + 2z)$	$G_0 = (20 + 2z)$
S2	$s_u = 0.75 \times (20 + 2z)$	$G_0 = 1.25 \times (20 + 2z)$
S3	$s_u = 0.75 \times (20 + 2z)$	$G_0 = (20 + 2z)$

Table 10. Suggested approaches for practical analysis

Analysis	Analysis description
Basic analysis	Details are specified in Figure 8.
F1	The following aspects are included in the analysis: stiffness reduction, soil/structure interface behaviour, thermal effect of concrete beams and floor slabs, joints in the diaphragm wall. The diaphragm wall and piles are modelled with solid elements, with soil/wall and soil/pile interface properties ($\tau_{\max} = 0.5 s_u$). The stiffness of the reinforced concrete components is reduced to half of the nominal stiffness ($R = 0.5$) to model the imperfections in the concrete. A temperature change ($\Delta T = -10K$) is applied to all levels of floor slabs and beams to consider thermal shrinkage during concrete curing process, and additional $\Delta T = -20K$ is applied to top floor slabs and beams only to consider ambient temperature change during winter. The diaphragm wall is modelled as a cross anisotropic linear elastic material ($\beta = 0.2$) to consider the effect of construction joints.
F2	The model of the soil/pile interface behaviour is removed from F1. The piles are modelled with beam elements, which is likely to be a more feasible approach for routine design calculations.
F3	The soil/wall and soil/pile interface models are removed from F1. The piles are modelled with beam elements.

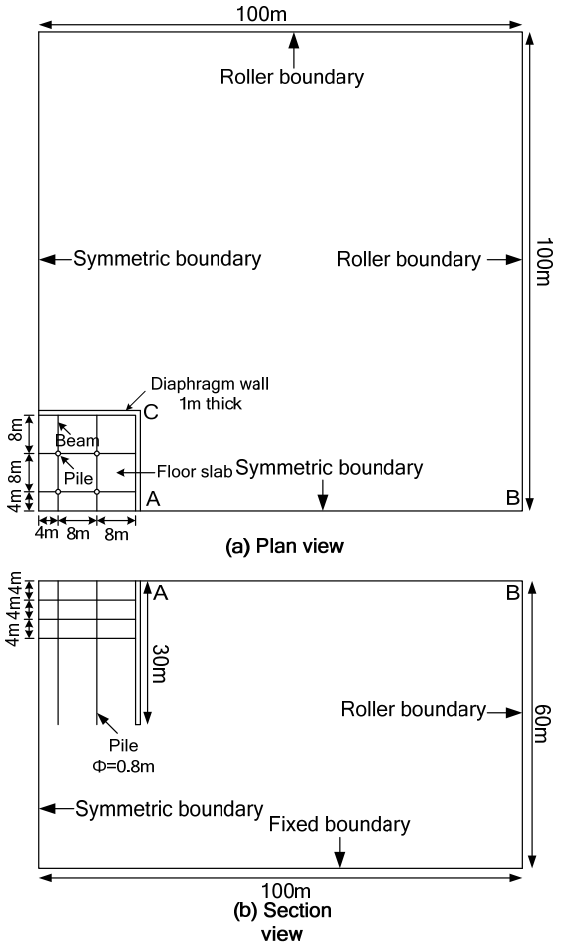

Figure 1. Geometric model of the supported deep excavation that is adopted for the parametric study

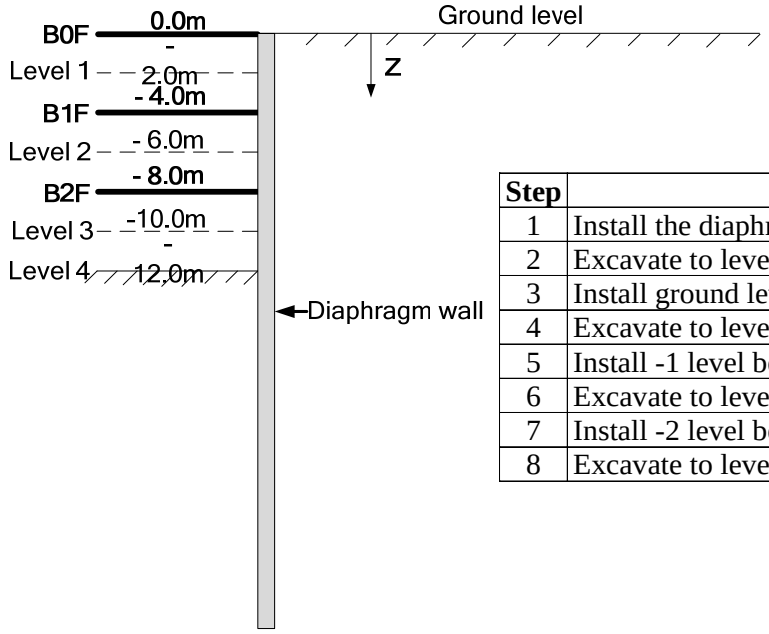

Step	Description
1	Install the diaphragm wall and piles.
2	Excavate to level 1 at -2m.
3	Install ground level beams and floor slabs (B0F).
4	Excavate to level 2 at -6m.
5	Install -1 level beams and floor slabs (B1F).
6	Excavate to level 3 at -10m.
7	Install -2 level beams and floor slabs (B2F).
8	Excavate to level 4 at -12m.

Figure 2. Top-down construction sequence

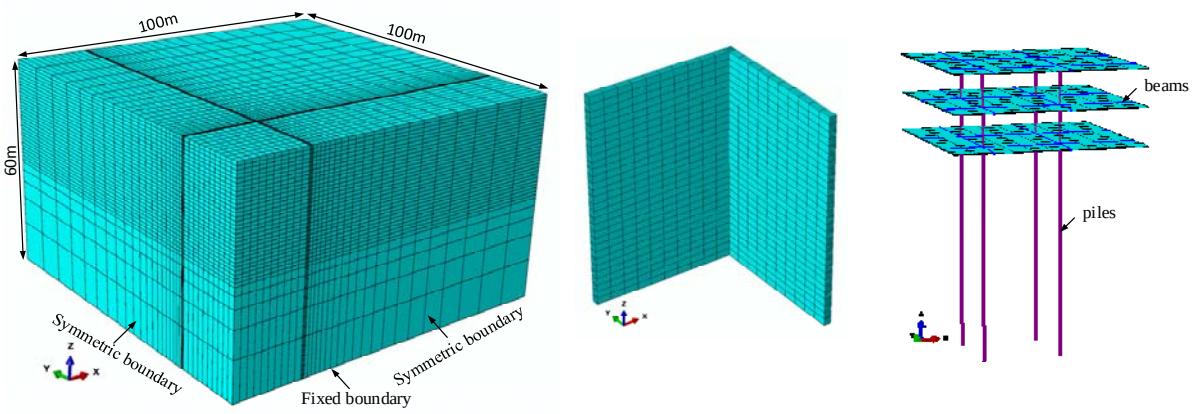

(a) The soil (piles modelled as beam elements)

(b) The wall (solid elements)

(c) Floor slabs, beams, and piles (beam elements)

Figure 3. Mesh for the soil and retaining structures in the basic analysis

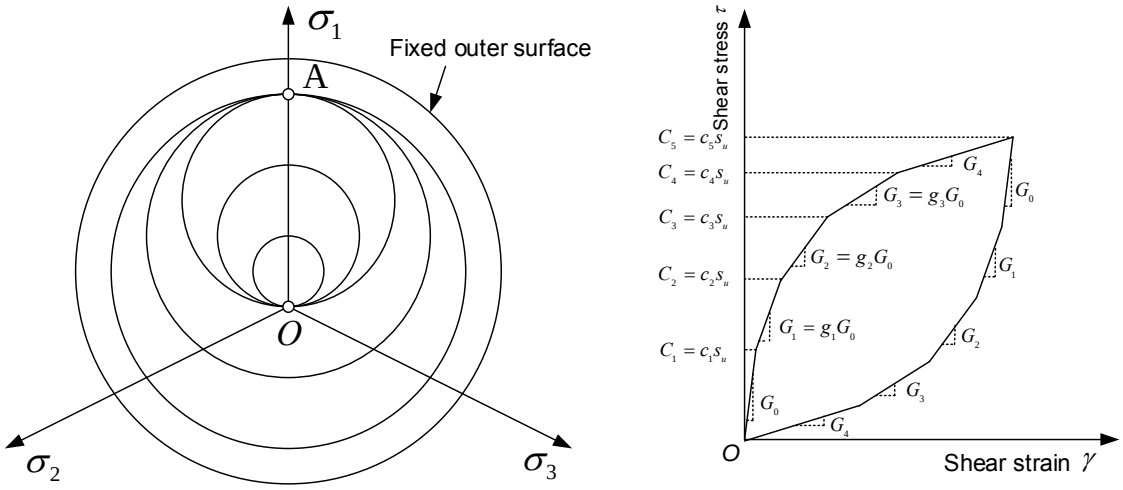

(a) Yield surfaces after stress path from O to A and back to O

(b) Shear stress-strain curve with stiffness degradation

Figure 4. Multiple yield surface kinematic hardening model, showing a loading path O to A followed by an unloading path A to O

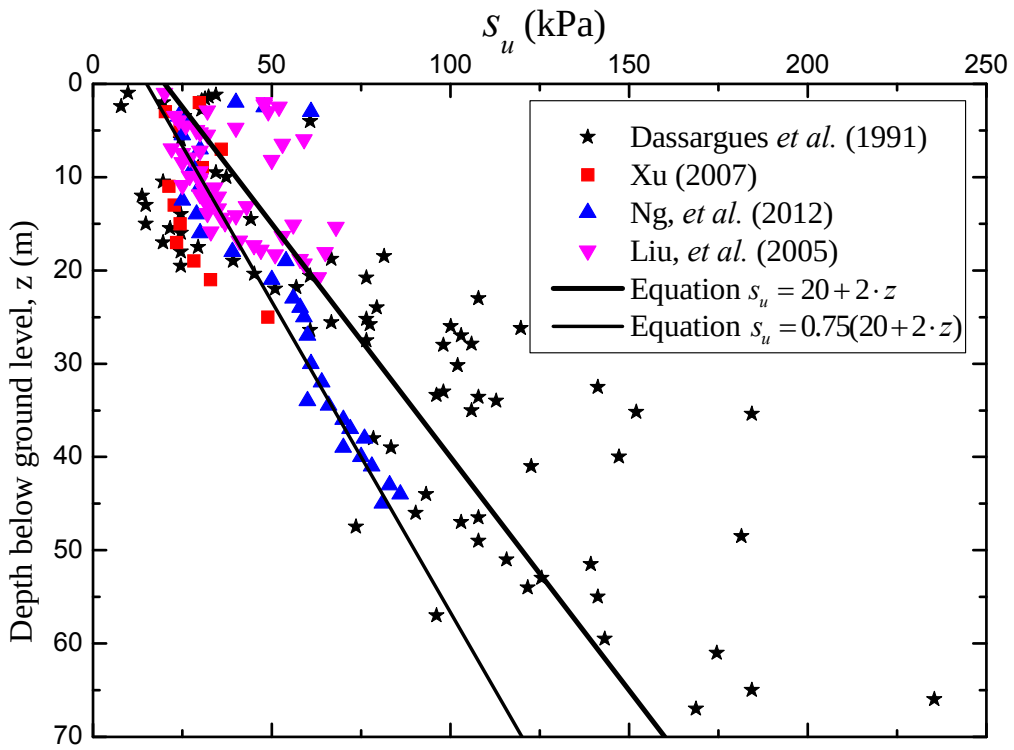

Figure 5. Undrained shear strength s_u profile for Shanghai Clay

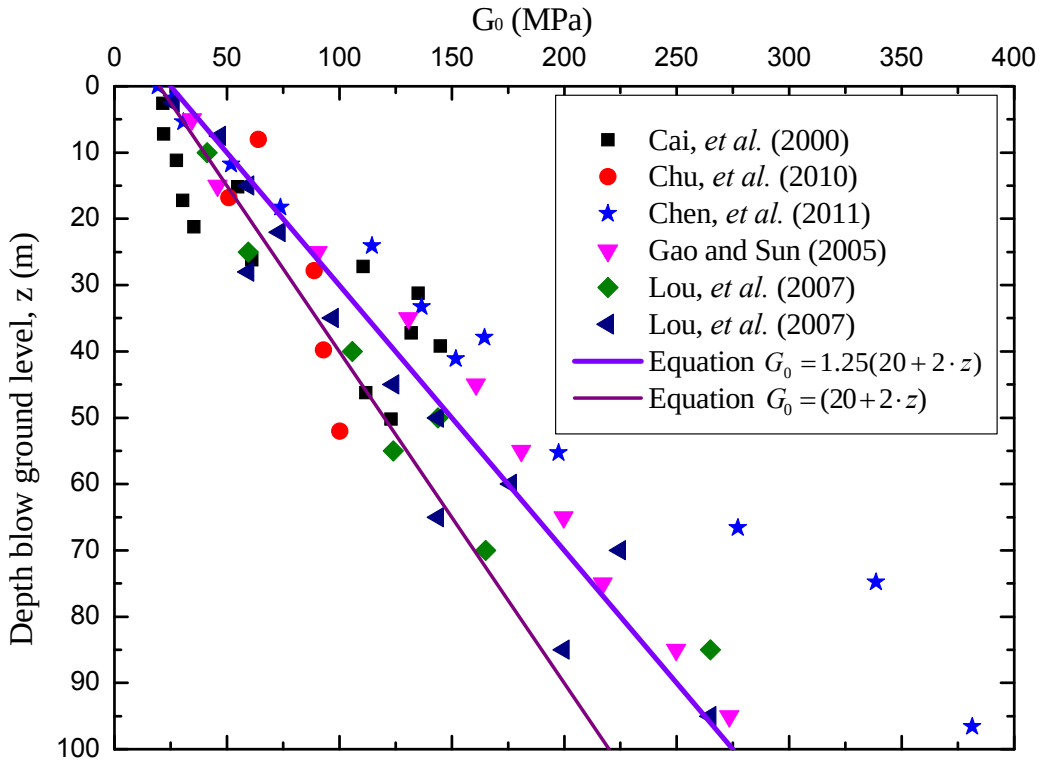

Figure 6. Shear modulus G_0 profile for Shanghai Clay

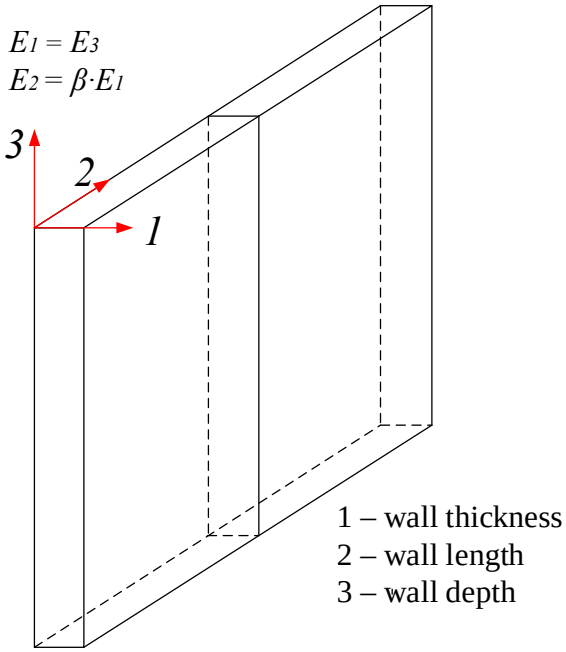

Figure 7. Local directions for cross anisotropic wall

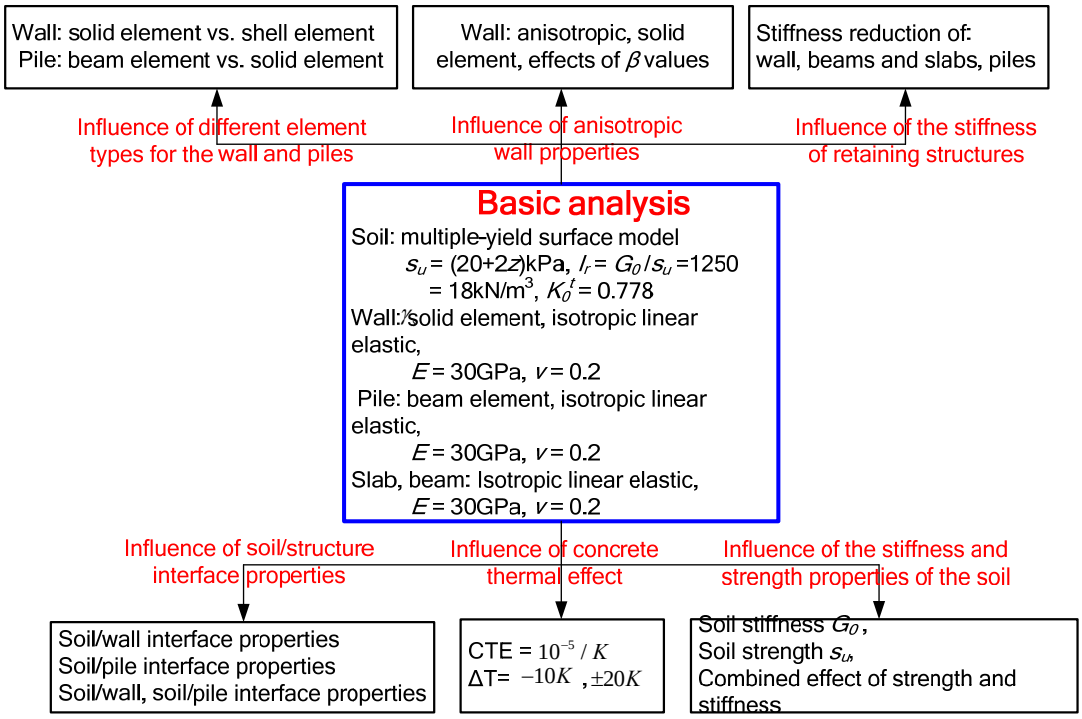

Figure 8. Parametric study

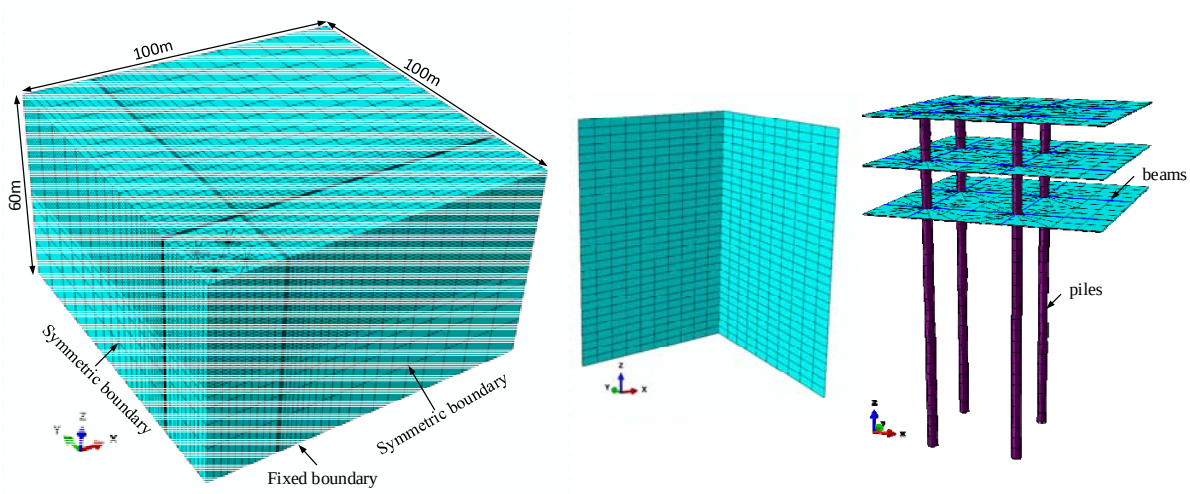

(a) The soil (piles modelled as beam elements) (b) The wall (shell elements) (c) Floor slabs, beams, and piles (solid elements)

Figure 9. Alternative meshes for soil and retaining structure (analyses E1 and E2)

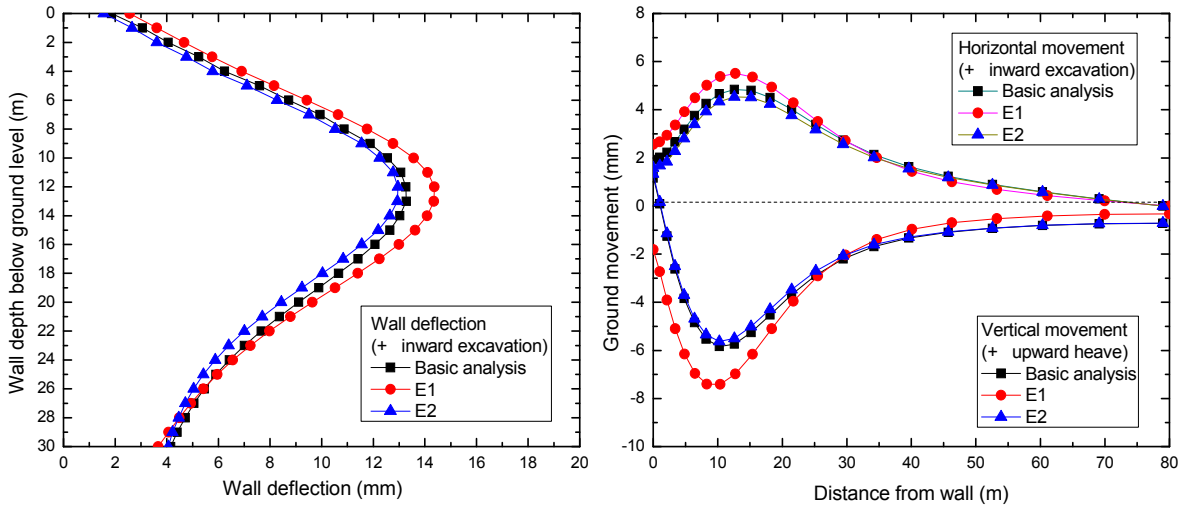

Figure 10. Wall deflection and ground movement (parametric study on element type)

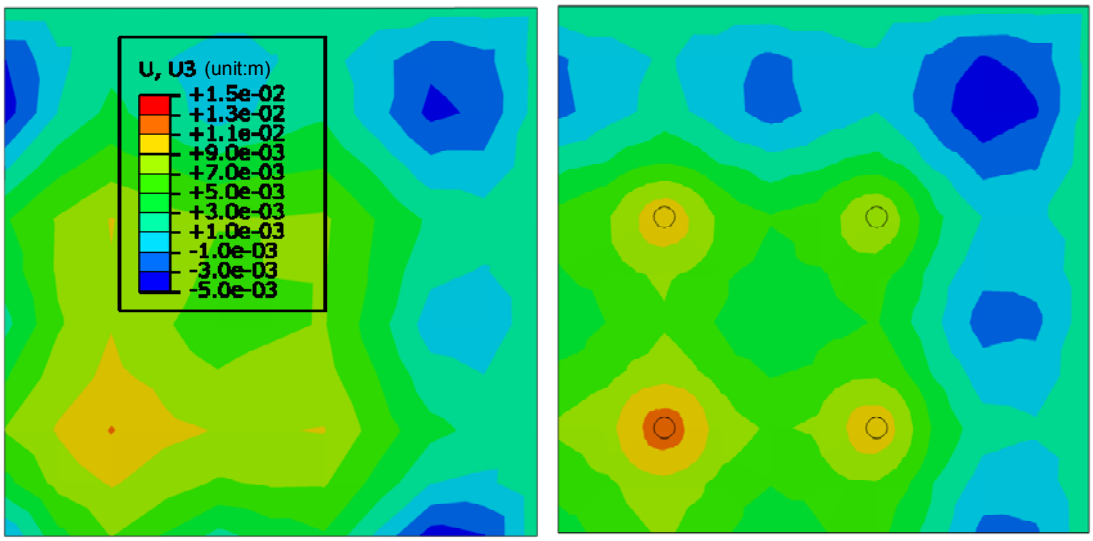

(a) Basic analysis (beam piles) (b) E2 (solid piles)

Figure 11. Vertical displacement contour of ground level floor slab (parametric study on element type)

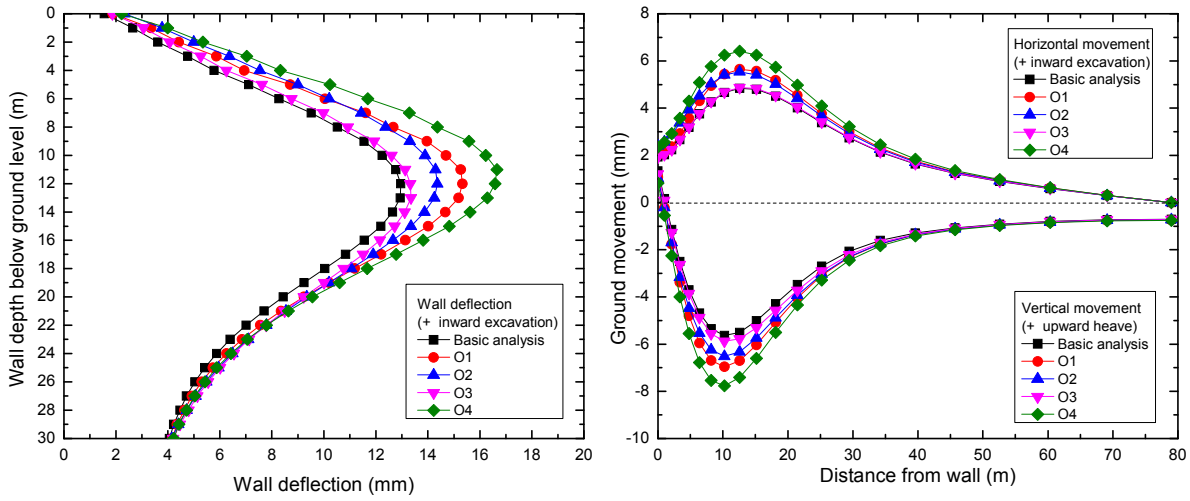

Figure 12. Wall deflection and ground movement (parametric study on operational stiffness)

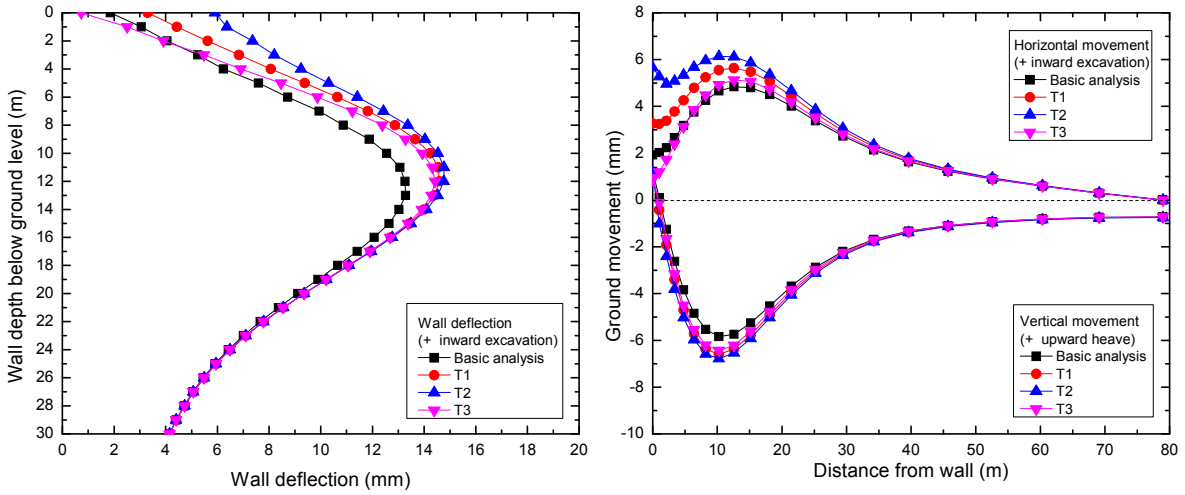

Figure 13. Wall deflection and ground movement (parametric study on thermal effects)

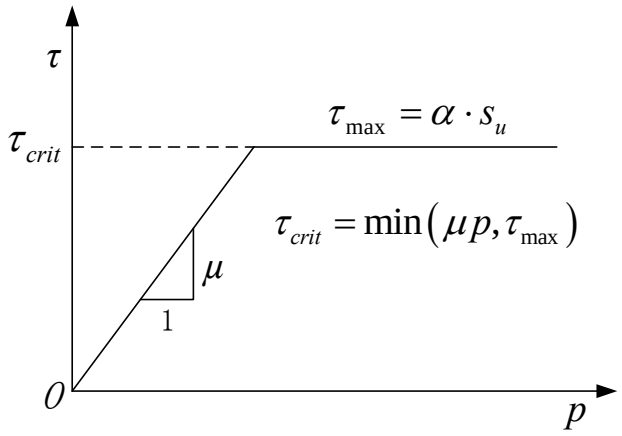

Figure 14. Extended Coulomb friction model

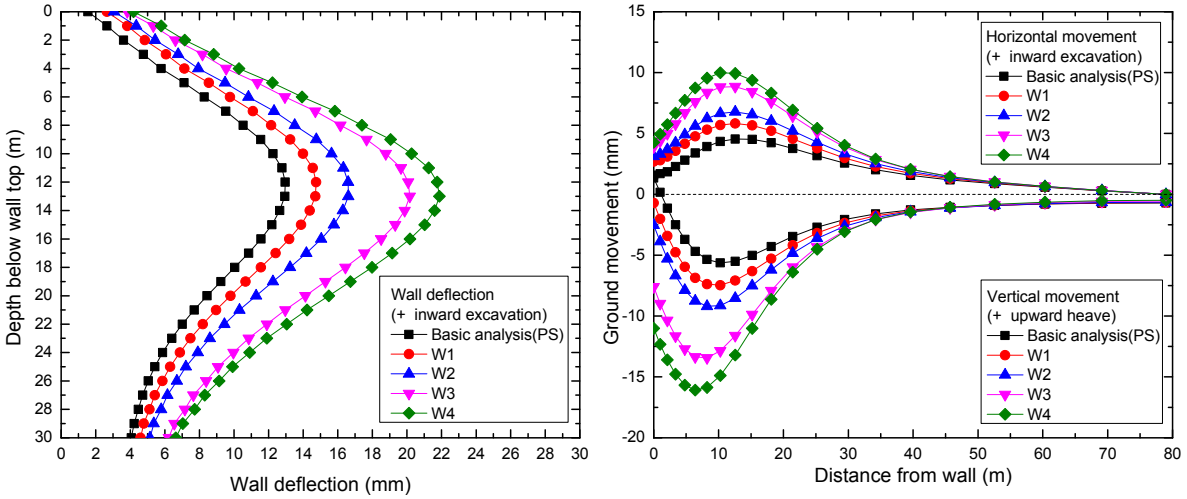

Figure 15. Wall deflection and ground movement (parametric study on soil/wall interface properties)

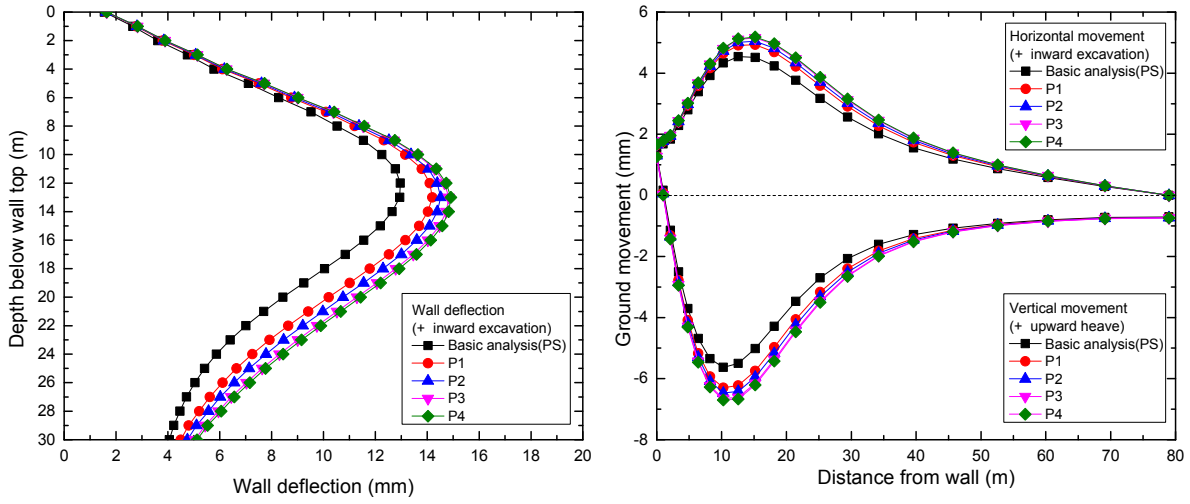

Figure 16. Wall deflection and ground movement (parametric study on the soil/pile interface)

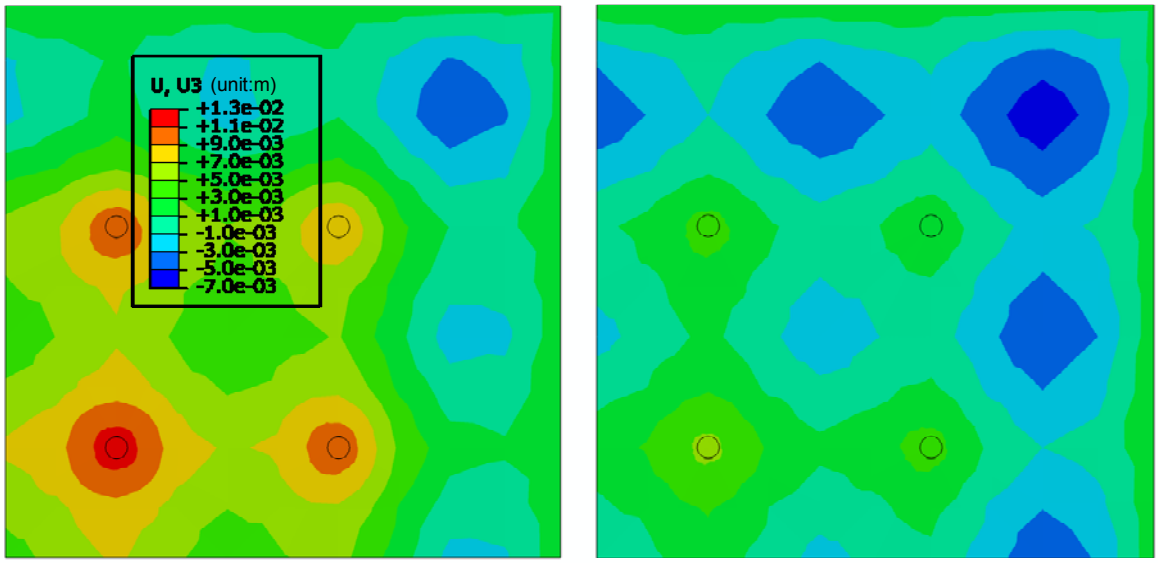

(a) Basic analysis(PS) (tied soil/pile interface)

(b) P4 (smooth soil/pile interface)

Figure 17. Vertical displacement of the ground level floor slab (parametric study on the soil/pile interface)

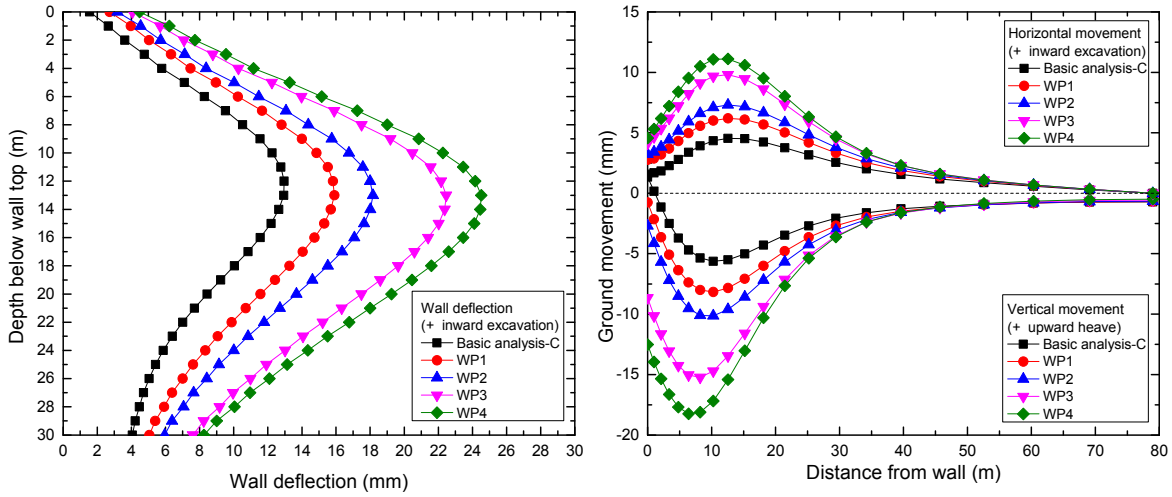

Figure 18. Wall deflection and ground movement (parametric study on combined soil/wall and soil/pile contact)

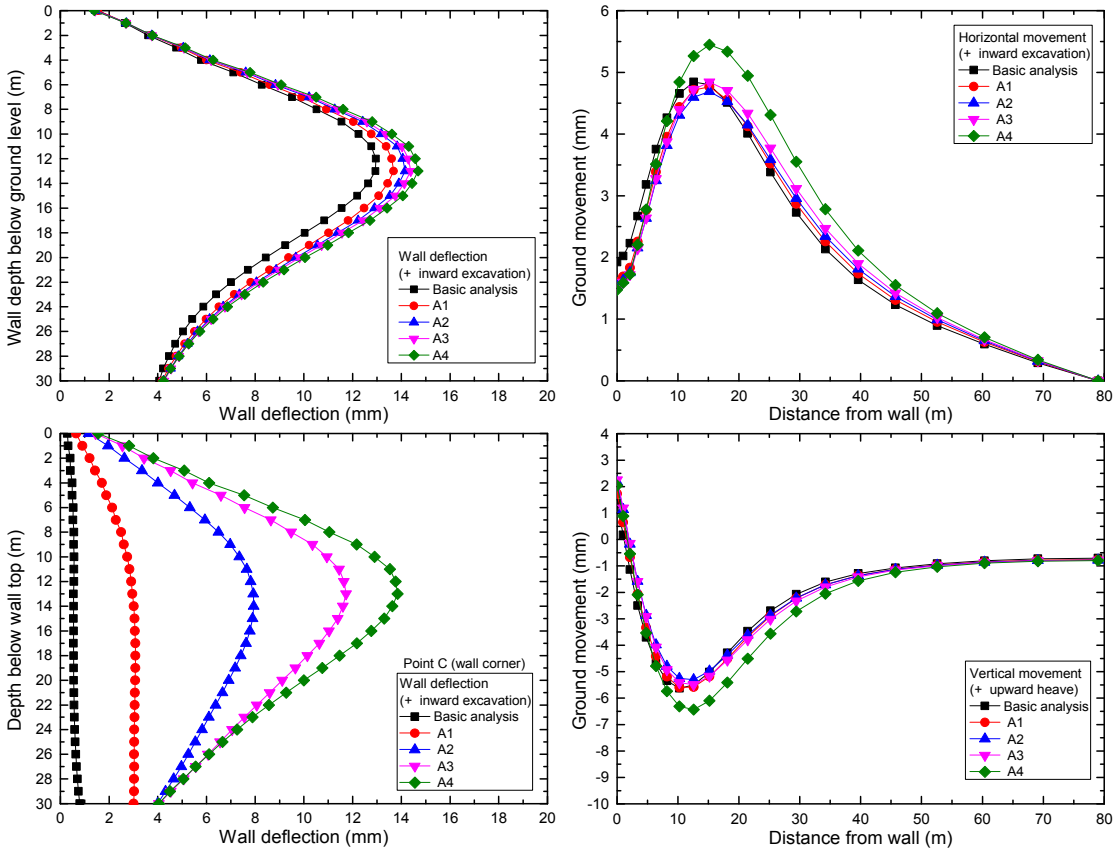

Figure 19. Wall deflection and ground movement (parametric study on wall anisotropy)

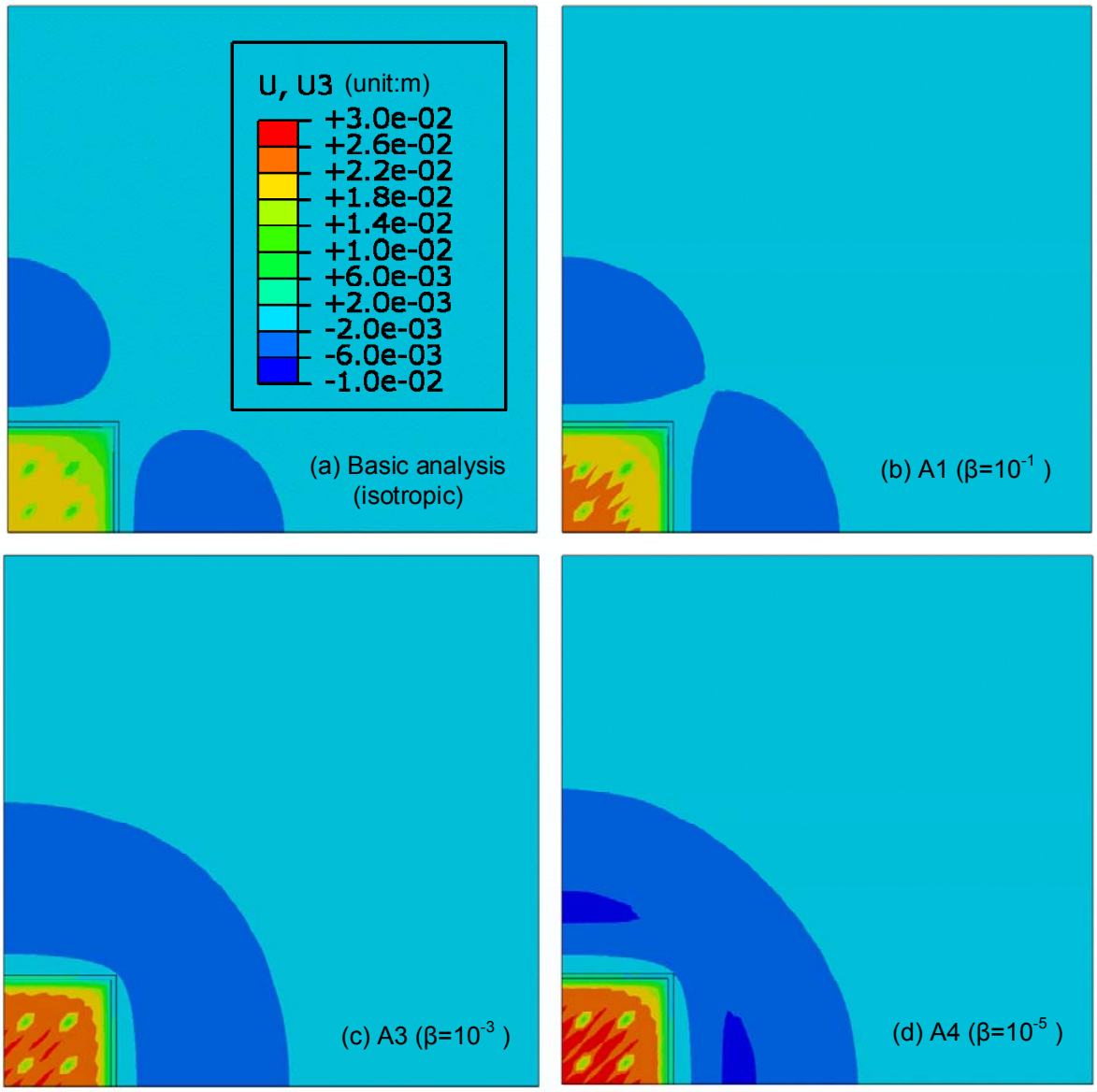

Figure 20. Ground vertical displacement in units of metres (parametric study on wall anisotropy)

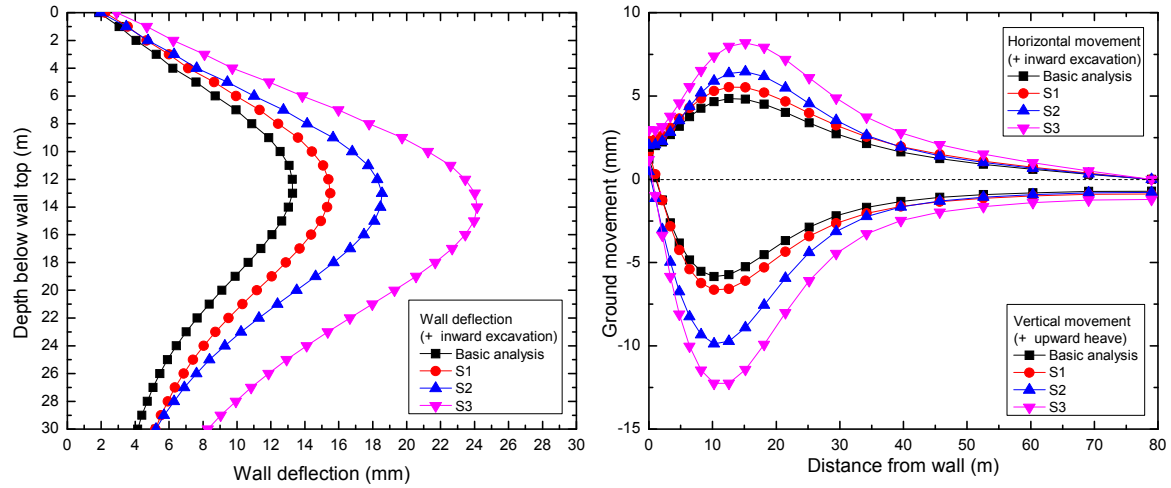

Figure 21. Wall deflection and ground movement (parametric study on soil properties)

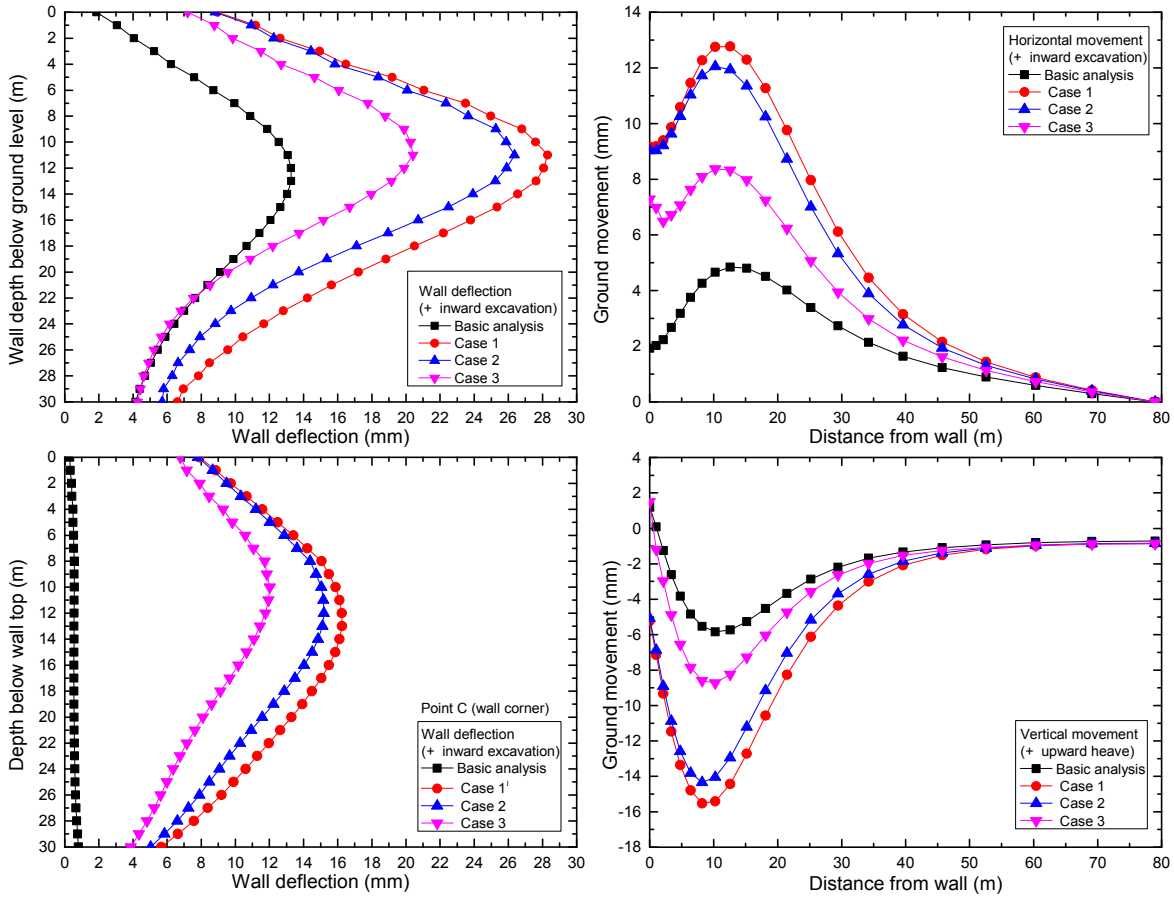

Figure 22. Wall deflection and ground movement (suggested approaches)

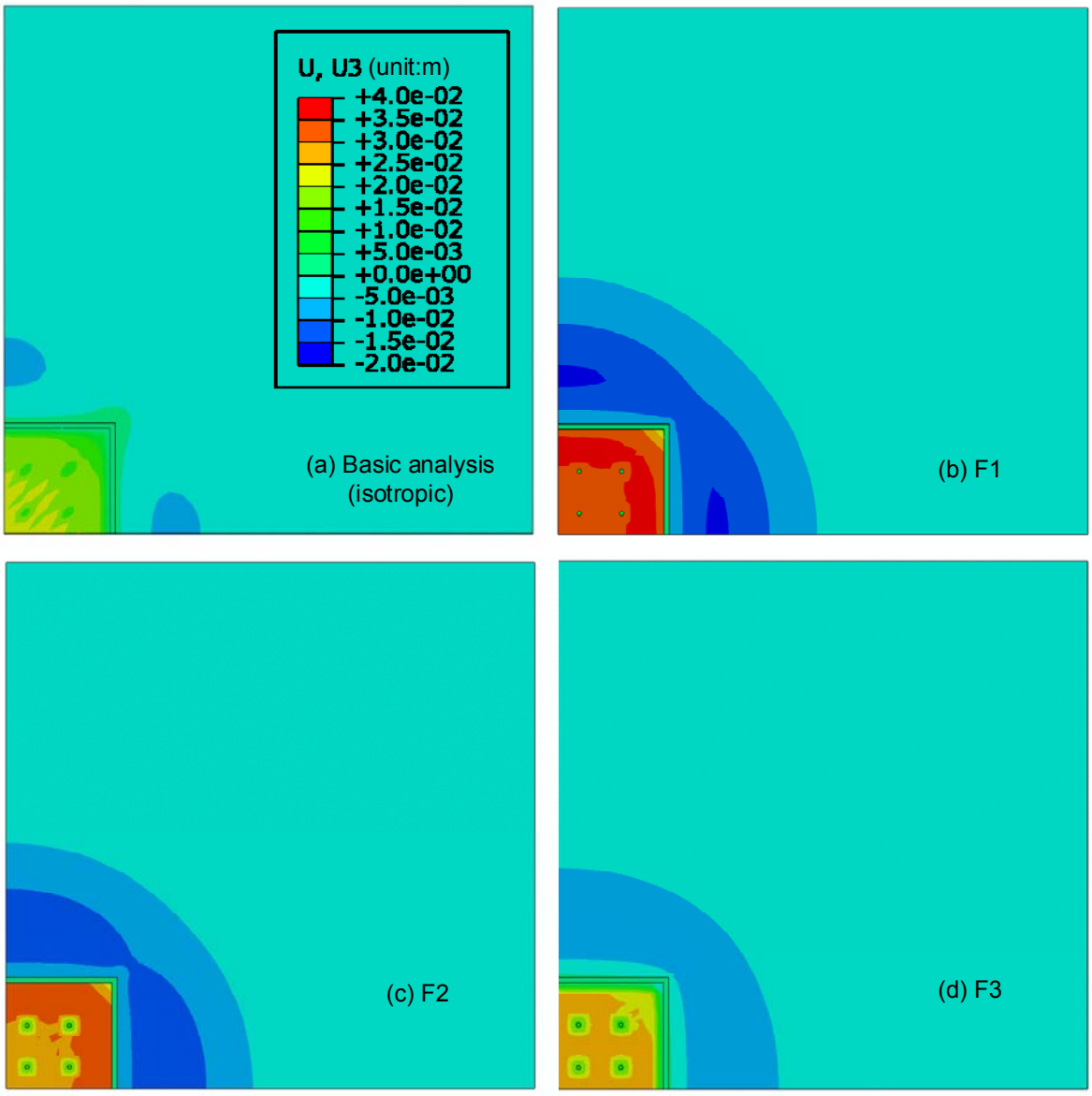

Figure 23. Vertical ground movement (suggested approaches)